Preprints of the 21st IFAC World Congress (Virtual)
Berlin, Germany, July 12-17, 2020

Pose Observation for Second Order Pose Kinematics ⋆

Yonhon Ng * **Pieter van Goor** * **Robert Mahony** *

* *Research School of Electrical, Energy and Materials Engineering, Australian National University, Acton ACT 2601, Australia (email: {yonhon.ng, pieter.vangoor,robert.mahony}@anu.edu.au)*

Abstract: This paper proposes an equivariant observer for second order pose estimation of a rigid body. The observer exploits the second order kinematic model and its symmetry group. The observer uses conventional sensors and simple computations that allow it to be run on resource-constrained devices. The observer design is based on the lifted kinematics and we prove its asymptotic convergence property. The performance of the observer is demonstrated in simulation.

Keywords: Estimation and filtering, Continuous time system estimation, second order kinematics, equivariant observer, symmetry group, virtual reality, augmented reality

1. INTRODUCTION

Robust estimation of pose and velocity is vital for many applications in Virtual Reality (VR), Augmented Reality (AR) and mobile robotics applications. In most of these applications, the device tends to have strict power, latency, computational and sensors constraints. In VR and AR community, vision sensor is a natural sensor modality since a camera provides an information rich measurement that enable interaction between real and virtual world. Hybrid systems that use vision and inertial sensor are the most promising configuration for indoor and outdoor applications (Hughes et al., 2005; Rabbi and Ullah, 2013; Marchand et al., 2015).

The classical method of nonlinear state estimation is based on some variant of the Extended Kalman Filter (EKF) (e.g., Bonnable et al. (2009); Barrau and Bonnabel (2016); Wu et al. (2017)). More recently, nonlinear observers (e.g., Mahony et al. (2008, 2009); Grip et al. (2011)) are becoming more popular. Nonlinear observers are generally simpler to implement for real-time applications. Additionally, nonlinear observers can guarantee powerful convergence properties, whereas similar results are challenging to prove for EKF designs. For these reasons, this work proposes a simple and efficient nonlinear observer, and proves asymptotic convergence.

Most existing work on observer design uses a first order system model, where the input to the system is the first time derivative of the variable to be estimated. For example, attitude estimation (e.g., Mahony et al. (2008); Grip et al. (2011); Hua et al. (2014); Liu and Zhu (2018)) uses gyroscope to measure the angular velocity, which is integrated and then corrected by vector measurements. Velocity-aided attitude estimation (e.g., Bonnable et al. (2009); Hua et al. (2016, 2017)) uses Inertial Measurement Unit (IMU) and linear velocity sensor (e.g., GPS, doppler sensor) to estimate the attitude and linear velocity. In this case, the linear velocity kinematics are first order to acceleration and the works do not consider the position estimation. Pose estimation (e.g., Baldwin et al. (2009); Hua et al. (2011, 2015); Hamel and Samson (2017); Hashim et al. (2019)) also assumes both linear and angular velocity can be directly measured. The recent work by Barrau and Bonnabel (2016) is also based on first order kinematics. Mahony et al. (2013) proposed equivariant observer that leverage the symmetric property of kinematics system. This allows the behaviour of the system to be analysed at one point, and transported to all points using symmetric transformation to obtain a global observer design. To the best of our knowledge, our previous paper (Ng et al., 2019) is the first work on second order equivariant observer.

In this paper, we extend our novel work (Ng et al., 2019) on the second order attitude kinematics to second order pose kinematics. An output equivariant pose observer for the second order pose kinematics is proposed. The observer uses linear and angular acceleration measurements as inputs to the second order pose kinematics. The innovation is constructed using measurements of the magnetic field direction and relative position measurements from the device to visible known landmarks. Most of the measurements can be obtained by conventional inertial measurement units (IMUs). The relative position measurement can be obtained using a monocular camera observing known 2D landmarks (e.g., ArUco marker), stereo cameras, or RGBD camera.

The paper is organised as follows. Section 1 presents the introduction and related work, Section 2 discusses the problem formulation which covers the state space and measurements used. Section 3 presents the symmetry group of the second order pose kinematics, the associated group action, and defines the origin point. Section 4 presents our proposed observer and stability analysis, followed by Section 5 where simulation results are shown

⋆ This work was partially supported by the Australian Research Council through the ARC Discovery Project DP160100783 "Sensing a complex world: Infinite dimensional observer theory for robots"

and discussed. Section 6 presents the conclusion and future work.

2. PROBLEM FORMULATION

This paper considers the problem of estimating the second order pose of a rigid body. We denote the pose as P, body-fixed velocity as V, and body-fixed acceleration as U such that

$$P = \begin{bmatrix} R & t \\ 0 & 1 \end{bmatrix} \in \mathbf{SE}(3),$$
$$V = \begin{bmatrix} \Omega^\times & v \\ 0 & 0 \end{bmatrix} \in \mathfrak{se}(3),$$
$$U = \begin{bmatrix} \theta^\times & a \\ 0^\top & 0 \end{bmatrix} \in \mathrm{T}\mathfrak{se}(3) \equiv \mathfrak{se}(3),$$

where $R \in \mathbf{SO}(3)$ and $t \in \mathbb{R}^3$ are the orientation and translation of the body-fixed frame with respect to the world fixed frame $\{W\}$, $\Omega^\times$ is the body-fixed angular velocity represented by a skew-symmetric matrix, v is the body-fixed linear velocity, $\theta^\times$ is the body-fixed angular acceleration represented by a skew-symmetric matrix, and a is the body-fixed linear acceleration.

Then, the classical second order pose kinematics is given by

$$\dot{P} = PV, \tag{1a}$$
$$\dot{V} = U. \tag{1b}$$

Note that unlike dynamics, we do not model mass, inertia and coriolis effects.

Next, we introduce the state and velocity spaces for the second-order pose kinematics. The second order pose kinematics are naturally posed on $\mathrm{T}\mathbf{SE}(3)$. By using the standard left trivialisation of the velocity space, a tangent vector $P_\xi V_\xi \in \mathrm{T}_{P_\xi}\mathbf{SE}(3)$ is identified with $V_\xi \in \mathfrak{se}(3)$. In this manner, we consider the state of our system as an element of the product manifold

$$\mathcal{M} = \mathbf{SE}(3) \times \mathfrak{se}(3).$$

The associated velocity space is the tangent $\mathrm{T}_{P_\xi}\mathbf{SE}(3)$ to $\mathbf{SE}(3)$ at $P_\xi \in \mathbf{SE}(3)$ and that tangent space $\mathrm{T}\mathfrak{se}(3)$ to $\mathfrak{se}(3)$ at a point $V_\xi \in \mathfrak{se}(3)$. Since $\mathfrak{se}(3)$ is a linear space, then $\mathrm{T}\mathfrak{se}(3) \equiv \mathfrak{se}(3)$. The tangent space $\mathrm{T}_{P_\xi}\mathbf{SE}(3)$ can be left trivialised to $\mathfrak{se}(3)$ analogously to the approach taken above. Thus, the input velocity space that we consider is based on this construction for a parametrization of the tangent space to $\mathcal{M}$. That is a space $\mathbb{V} = \mathfrak{se}(3) \times \mathrm{T}\mathfrak{se}(3)$ where we preserve the $\mathrm{T}\mathfrak{se}(3)$ notation to make clear the part of the velocity space that is modelling the second order part of the kinematics. An element $u = (U_1, U_2) \in \mathbb{V} \equiv \mathfrak{se}(3) \times \mathrm{T}\mathfrak{se}(3)$ in the input space can be thought of as two independent elements $U_1 \in \mathfrak{se}(3)$ and $U_2 \in \mathrm{T}\mathfrak{se}(3) \equiv \mathfrak{se}(3)$.

For an element $\xi = (P_\xi, V_\xi) \in \mathcal{M}$, and velocity $u = (U_1, U_2) \in \mathbb{V} \equiv \mathfrak{se}(3) \times \mathrm{T}\mathfrak{se}(3)$, the kinematics are given by

$$\dot{P}_\xi = P_\xi(V_\xi + U_1), \tag{2a}$$
$$\dot{V}_\xi = U_2, \tag{2b}$$

and the kinematics system of the state is

$$\dot{\xi} = f(\xi, u) = (P_\xi(V_\xi + U_1), U_2). \tag{3}$$

Note that the natural behaviour of the system is recovered by measuring the linear and angular acceleration input in U_2 and by setting $U_1 \equiv 0$. That is, the velocity input U_1 that acts on the first order state kinematics is zero in the natural system kinematics (as in (1)). A key property of the kinematics (2) is the presence of the drift term

$$f((P_\xi, V_\xi), 0) = (P_\xi V_\xi, 0)$$

for $u \equiv 0 \in \mathbb{V}$. That is, the system function is affine in the input $u \in \mathfrak{se}(3) \times \mathrm{T}\mathfrak{se}(3)$ similar to the novel work on second order attitude kinematics discussed in Ng et al. (2019).

The first component of the state $\xi = (P_\xi, V_\xi) \in \mathbf{SE}(3) \times \mathfrak{se}(3)$ is the pose P_ξ of the rigid body with respect to an inertial frame. The second component of the state is the linear and angular velocity V_ξ expressed in the body-fixed frame $\{B\}$. The input u for the system kinematics in (3) contains the input velocity U_1 and the input acceleration U_2 of the rigid body with respect to the inertial frame, expressed in the body fixed frame $\{B\}$.

In the subsequent sections, we use the following notation to represent homogeneous coordinates

$$\overline{v} = \begin{bmatrix} v \\ 1 \end{bmatrix}, \qquad \hat{\overline{v}} = \begin{bmatrix} v \\ 0 \end{bmatrix}.$$

2.1 Measurement of Input Acceleration

An accelerometer is used to measure the linear acceleration of the rigid body. Following non-rotating, flat Earth assumption, the acceleration of the body-fixed frame a_B can be obtained from the accelerometer measurement, a and gravitational acceleration, $a_G = [0, 0, 9.81]^\top$ as follows (Hua and Allibert, 2018)

$$\hat{\overline{a}}_B = \hat{\overline{a}} - {P_\xi}^{-1}\hat{\overline{a}}_G - \Omega \times v. \tag{4}$$

If the rigid body has at least four non-coplanar accelerometers placed at known locations, similar to Ng et al. (2019), the angular acceleration $\theta^\times$ of the rigid body can also be recovered. The input acceleration is then

$$U_2 = \begin{bmatrix} \theta^\times & a_B \\ 0^\top & 0 \end{bmatrix}. \tag{5}$$

2.2 Partial Measurement of Pose

The pose of the rigid body can be partially observed by using a vision sensor (camera) looking at landmarks placed at known location in the scene. We assume each visible landmark can provide a relative pose between the camera and the visible landmark. We denote the position of the landmark relative to the inertial frame as p_i°, the measured relative position relative to the camera as p_i, such that $p_i^\circ, p_i \in \mathbb{R}^3$. Then,

$$\overline{p}_i = {P_\xi}^{-1}\overline{p}_i^\circ. \tag{6}$$

A single visible landmark will constraint the possible pose to any point on a sphere with fixed radius, and an unknown rotation around the line joining the landmark and the camera (3 degrees of freedom). Two landmarks will constraint the possible pose to any point on a circle (1 degree of freedom). Three or more visible landmarks will fully constraint the pose to a single solution.

2.3 Partial Measurement of Orientation

The orientation can be partially observed by using a magnetometer, and assuming that the magnetic field remains constant and known throughout the experiment. This constraints the orientation of the rigid body with only an ambiguity around the direction of the magnetic field. We denote the magnetic field direction relative to the inertial frame by m°, the measured magnetic field direction in body-fixed frame by m, such that $m^\circ, m \in S^2 \subset \mathbb{R}^3$. Then,

$$\overset{\circ}{m} = {P_\xi}^{-1}\overset{\circ}{m}^\circ. \tag{7}$$

3. SYMMETRY OF POSE SYSTEM

Physical systems usually have physical models with symmetries that encode the equivariance of the laws of motion. When viewed through a symmetric transformation of space, the behaviour of the system at one point is the same as the behaviour at another point in the state space. Thus, a system with symmetry allows a global analysis of an observer by analysing the behaviour at one point in space (Mahony et al., 2013; Ng et al., 2019).

3.1 The Symmetry Group

The symmetry group $\mathbf{G}$ we consider is a semi-direct product of $\mathbf{SE}(3) \ltimes \mathfrak{se}(3)$. Let two elements in the symmetry group be (A, a) and (B, b). Then, following Brockett and Sussmann (1972), the semi-direct group product is given by

$$(A, a) \cdot (B, b) = (AB, a + \mathrm{Ad}_A\, b), \tag{8}$$

with group identity $(I_4, 0)$ and group inverse

$$(A, a)^{-1} = (A^{-1}, -\mathrm{Ad}_{A^{-1}}\, a). \tag{9}$$

Define a map $\phi : \mathbf{G} \times \mathcal{M} \to \mathcal{M}$ by

$$\phi((A, a), (P_\xi, V_\xi)) = (P_\xi A, \mathrm{Ad}_{A^{-1}}(V_\xi - a)). \tag{10}$$

Lemma 3.1. The action ϕ (10) is a transitive right group action of $\mathbf{G}$ on $\mathcal{M}$.

Proof. Let $(A, a), (B, b) \in \mathbf{G}$. Then,

$$\begin{aligned}
\phi((A,a),&\phi((B,b),(P_\xi,V_\xi))) \\
&= \phi((A,a),(P_\xi B, \mathrm{Ad}_{B^{-1}}(V_\xi - b))) \\
&= (P_\xi BA, \mathrm{Ad}_{A^{-1}}(\mathrm{Ad}_{B^{-1}}(V_\xi - b) - a)) \\
&= (P_\xi BA, \mathrm{Ad}_{A^{-1}B^{-1}}(V_\xi - b - \mathrm{Ad}_B\, a)) \\
&= (P_\xi (BA), \mathrm{Ad}_{(BA)^{-1}}(V_\xi - (b + \mathrm{Ad}_B\, a))) \\
&= \phi((B,b)\cdot(A,a),(P_\xi,V_\xi)).
\end{aligned}$$

This demonstrates that the (right handed) group action property holds. It is straightforward to verify that $\phi((I_4, 0), (P_\xi, V_\xi)) = (P_\xi, V_\xi)$.

To see that ϕ is transitive, let (P_ξ, V_ξ) and (P'_ξ, V'_ξ) be any elements of $\mathcal{M}$. Then we can find the group element $({P_\xi}^{-1}P'_\xi, V_\xi - \mathrm{Ad}_{{P_\xi}^{-1}P'_\xi} V'_\xi)$ such that

$$\begin{aligned}
&\phi(({P_\xi}^{-1}P'_\xi, V_\xi - \mathrm{Ad}_{{P_\xi}^{-1}P'_\xi} V'_\xi), (P_\xi, V_\xi)) \\
&\quad = (P_\xi {P_\xi}^{-1} P'_\xi, \mathrm{Ad}_{{P'_\xi}^{-1}P_\xi}(V_\xi - (V_\xi - \mathrm{Ad}_{{P_\xi}^{-1}P'_\xi} V'_\xi))) \\
&\quad = (P'_\xi, V'_\xi).
\end{aligned}$$

□

3.2 Output Equivariance

Define a map $\rho^i : \mathbf{G} \times \mathcal{N}_i \to \mathcal{N}_i$ by

$$\rho^i((A, a), \overline{y}_i) = A^{-1}\overline{y}_i, \tag{11}$$

where $\mathcal{N}_i \equiv \mathbb{R}^4$ representing a homogeneous coordinate.

Lemma 3.2. The map ρ^i (11) is a transitive right group action of $\mathbf{G}$ on $\mathcal{N}_i$. Moreover, the measurement function h is equivariant with respect to actions ϕ (10) and ρ^i. That is

$$\rho^i_X(h(\xi)) = h^i(\phi_X(\xi)).$$

Proof. Let $(A, a), (B, b) \in \mathbf{G}$ and let $\overline{y}_i \in \mathcal{N}_i$. Then we have

$$\begin{aligned}
\rho^i((A,a),\rho^i((B,b),\overline{y}_i)) &= \rho^i((A,a),B^{-1}\overline{y}_i)), \\
&= A^{-1}B^{-1}\overline{y}_i, \\
&= (BA)^{-1}\overline{y}_i, \\
&= \rho^i((B,b)\cdot(A,a),\overline{y}_i).
\end{aligned}$$

This shows that the (right handed) group action property holds. It is straightforward to verify that $\rho^i((I_4, 0), \overline{y}_i) = \overline{y}_i$. Thus, ρ is indeed a right action.

$$\begin{aligned}
h^i(\phi_X(\xi)) &= h^i((P_\xi A, \mathrm{Ad}_{A^{-1}}(V_\xi - a))) \\
&= (P_\xi A)^{-1}\overline{y}_i^\circ \\
&= A^{-1}{P_\xi}^{-1}\overline{y}_i^\circ \\
&= \rho^i_X(h^i(\xi)).
\end{aligned}$$

Thus, the measurement function h is verified to be equivariant with respect to action ϕ and ρ^i. □

3.3 System Lift onto the Group

In order to work with our observer on $\mathbf{G}$, we need to lift the kinematics of the system. A lifted equivariant system is defined as the system on the symmetry group $\mathbf{G}$

$$\dot{X} := \mathrm{d}L_X \Lambda(\xi, u), \tag{12a}$$

$$\overline{y}_i := \rho^i(X, \overline{y}_i^\circ) =: H_i(\xi), \tag{12b}$$

for $\xi \in \mathcal{M}$, $u \in \mathbb{V}$ and $\mathrm{d}L_X$ given by Lemma A.1.

Specifically, we require a system lift, which is a function $\Lambda : \mathcal{M} \times \mathbb{V} \to \mathfrak{g}$ such that $\mathrm{d}\phi_\xi[\Lambda(\xi, u)] = f(\xi, u)$ for all $\xi \in \mathcal{M}$, $u \in \mathbb{V}$. Define a function $\Lambda : \mathcal{M} \times \mathbb{V} \to \mathfrak{g}$ by

$$\Lambda((P_\xi, V_\xi), (U_1, U_2)) = (V_\xi + U_1, \left[V_\xi, U_1\right] - U_2), \tag{13}$$

where the square bracket represents the matrix commutator.

Lemma 3.3. The function Λ (13) is a lift function for (3) onto the group $\mathbf{G}$.

Proof. In order to show that $\Lambda(\xi, u)$ is indeed a system lift, we need to show that $\mathrm{d}\phi_\xi[\Lambda(\xi, u)] = f(\xi, u)$ for all $\xi \in \mathcal{M}$, $u \in \mathbb{V}$, and $X \in \mathbf{G}$. Let $(P_\xi, V_\xi) \in \mathcal{M}$, $(U_1, U_2) \in \mathbb{V}$, and $(A, a) \in \mathbf{G}$ be arbitrary.

Then we have

$$
\begin{aligned}
&\mathrm{d}\phi_{(P_\xi,V_\xi)}[\Lambda((P_\xi,V_\xi),(U_1,U_2))]\\
&\quad=\mathrm{D}_{(A,a)}\Big|_{I,0}(P_\xi A,\mathrm{Ad}_{A^{-1}}(V_\xi-a))[\Lambda((P_\xi,V_\xi),(U_1,U_2))]\\
&\quad=(P_\xi(V_\xi+U_1),-\Big[V_\xi+U_1,V_\xi\Big]-(\Big[V_\xi,U_1\Big]-U_2))\\
&\quad=(P_\xi(V_\xi+U_1),U_2)\\
&\quad=f((P_\xi,V_\xi),(U_1,U_2)),
\end{aligned}
$$

which shows that our condition holds, and therefore $\Lambda(\xi,u)$ is a system lift as required. □

3.4 Origin of the Global Coordinate

Let an element of the lifted state space be represented as $X=(A,a)\in\mathbf{G}$, with unknown initial condition $X(0)\in\mathbf{G}$. We denote a world fixed frame as $\{W\}$. It is necessary to pick a reference point $\xi^\circ=(P_{\xi^\circ},V_{\xi^\circ})\in\mathcal{M}$ with respect to $\{W\}$, which we term the *origin point*. This point defines an arbitrary origin for the global coordinate parametrization $\phi_{\xi^\circ}:\mathbf{G}\to\mathcal{M}$ of the state space $\mathcal{M}$ by the symmetry group $\mathbf{G}$. From Lemma 2 of (Mahony et al., 2013), the solution $X(t,X(0))$ projects back to the state $\xi(t,\xi^\circ)$ via the group action

$$\phi_{\xi^\circ}(X(t;X(0)))=\xi(t;\xi^\circ),$$

such that

$$
\begin{aligned}
(P_\xi,V_\xi)&=\phi((A,a),(P_{\xi^\circ},V_{\xi^\circ}))\\
&=(P_{\xi^\circ}A,\mathrm{Ad}_{A^{-1}}(V_{\xi^\circ}-a)),
\end{aligned}\tag{14}
$$

and,

$$
\begin{aligned}
(\hat{P}_\xi,\hat{V}_\xi)&=\phi((\hat{A},\hat{a}),(P_{\xi^\circ},U_0))\\
&=(P_{\xi^\circ}\hat{A},\mathrm{Ad}_{\hat{A}^{-1}}(V_{\xi^\circ}-\hat{a})).
\end{aligned}\tag{15}
$$

From equation (13) and (12a), the lifted kinematics on $\mathbf{G}$ can be written as

$$\dot{A}=A(\mathrm{Ad}_{A^{-1}}(V_{\xi^\circ}-a)+U_1),\tag{16a}$$

$$\dot{a}=\mathrm{Ad}_A(\Big[\mathrm{Ad}_{A^{-1}}(V_{\xi^\circ}-a),U_1\Big]-U_2),\tag{16b}$$

where $U_1\equiv 0$ in the real system, since there is no input linear and angular velocity (unlike first order state kinematics).

We denote the output associated to the chosen origin point to be

$$\overline{y}_i^\circ:=h^i(\xi^\circ).$$

4. OBSERVER DESIGN

Our proposed observer works on the symmetry group of the pose state space i.e. $\mathbf{G}$, and not the manifold $\mathcal{M}$. We use $\hat{X}(t;\hat{X}(0))\in\mathbf{G}$ to denote the estimate for the lifted system state $X(t;X(0))$ for unknown $X(0)$. The fundamental structure for the observer that we consider is that of a *pre-observer* (a copy of (16)) with innovation. The innovation takes outputs $\{\overline{y}_i\}$ and the observer state $\hat{X}$, and generates a correction term for the observer dynamics with the goal that $\hat{\xi}=\phi(\hat{X},\xi^\circ)$ converges to $\xi(t,\xi^\circ)$.

4.1 Proposed Observer

Theorem 4.1. Let $(P_{\xi^\circ},V_{\xi^\circ})$ be the chosen reference point in $\mathcal{M}$. Let $\hat{X}=(\hat{A},\hat{a})\in\mathbf{G}$, with arbitrary initial condition $\hat{X}(0)=(\hat{A}_0,\hat{a}_0)$. Consider the observer kinematics on the open-loop kinematics (16) with $U_1=0$ as

$$\dot{\hat{A}}=\hat{A}(\mathrm{Ad}_{\hat{A}^{-1}}(V_{\xi^\circ}-\hat{a}))-\Delta_1\hat{A},\tag{17a}$$

$$\dot{\hat{a}}=-\mathrm{Ad}_{\hat{A}}(U_2)-\Delta_2,\tag{17b}$$

where U_2 is given by (5) and

$$
\begin{aligned}
\Delta_1&=-k_1\,\mathrm{Ad}_{\hat{A}}(\mathbb{P}_{\mathfrak{se}(3)}\Big(M\Big)),\\
\Delta_2&=\mathrm{Ad}_{\hat{A}}(\mathbb{P}_{\mathfrak{se}(3)}\Big(\Big[\hat{V}_\xi,\mathrm{Ad}_{\hat{A}^{-1}}\Delta_1\Big]+k_2M\Big)),\\
M&=\sum_{i=1}^{N}\frac{1}{N}\hat{A}^\top\left(\overline{p}_i^\circ-\hat{A}\overline{p}_i\right)\overline{p}_i{}^\top+\hat{A}^\top\left(\overline{\overline{m}}^\circ-\hat{A}\overline{\overline{m}}\right)\overline{\overline{m}}^\top.
\end{aligned}
$$

Then, $(\hat{P}_\xi,\hat{V}_\xi)=\phi((\hat{A},\hat{a}),(P_{\xi^\circ},V_{\xi^\circ}))$ converges asymptotically to (P_ξ,V_ξ).

Proof. The stability of the observer (17) is analysed as follows. The Lyapunov function is defined as

$$\mathcal{L}=l^l+l^m+l^v,\tag{18}$$

and

$$
\begin{aligned}
l^l&=\sum_{i=1}^{N}\frac{1}{2N}\left|\overline{p}_i^\circ-\rho^i_{\hat{X}^{-1}}(\overline{p}_i)\right|^2,\\
l^m&=\frac{1}{2}\left|\overline{\overline{m}}^\circ-\rho^i_{\hat{X}^{-1}}(\overline{\overline{m}})\right|^2,\\
l^v&=\frac{1}{2k_2}\left\|V_\xi-\hat{V}_\xi\right\|_F^2,
\end{aligned}
$$

where $\|P\|_F=\sqrt{\mathrm{tr}\,(P^\top P)}$ denotes the Frobenius norm of a matrix, and $|p|=\sqrt{p^\top p}$ denotes the Euclidean norm of a vector.

Computing the time derivative of each components in (18),

$$
\begin{aligned}
\dot{l}^l&=\sum_{i=1}^{N}\frac{1}{N}\,\mathrm{tr}\left((\mathrm{Ad}_{\hat{A}^{-1}}\Delta_1)^\top\hat{A}^\top(\overline{p}_i^\circ-\hat{A}\overline{p}_i)\overline{p}_i{}^\top\right)\\
&\quad+\sum_{i=1}^{N}\frac{1}{N}\,\mathrm{tr}\left((V_\xi-\hat{V}_\xi)^\top\hat{A}^\top(\overline{p}_i^\circ-\hat{A}\overline{p}_i)\overline{p}_i{}^\top\right),
\end{aligned}\tag{19a}
$$

$$
\begin{aligned}
\dot{l}^m&=\mathrm{tr}\left((\mathrm{Ad}_{\hat{A}^{-1}}\Delta_1)^\top\hat{A}^\top(\overline{\overline{m}}^\circ-\hat{A}\overline{\overline{m}})\overline{\overline{m}}^\top\right)\\
&\quad+\mathrm{tr}\left((V_\xi-\hat{V}_\xi)^\top\hat{A}^\top(\overline{\overline{m}}^\circ-\hat{A}\overline{\overline{m}})\overline{\overline{m}}^\top\right),
\end{aligned}\tag{19b}
$$

$$\dot{l}^v=\frac{1}{k_2}\,\mathrm{tr}\left((V_\xi-\hat{V}_\xi)^\top(\Big[\hat{V}_\xi,\mathrm{Ad}_{\hat{A}^{-1}}\Delta_1\Big]-\mathrm{Ad}_{\hat{A}^{-1}}\Delta_2)\right).\tag{19c}$$

Combining (19a)(19b)(19c), the time derivative of the Lyapunov function is

$$
\begin{aligned}
\dot{\mathcal{L}}&=\Big\langle\,\mathrm{Ad}_{\hat{A}^{-1}}\Delta_1,M\Big\rangle\\
&\quad+\Big\langle V_\xi-\hat{V}_\xi,M+\frac{1}{k_2}(\Big[\hat{V}_\xi,\mathrm{Ad}_{\hat{A}^{-1}}\Delta_1\Big]-\mathrm{Ad}_{\hat{A}^{-1}}\Delta_2)\Big\rangle,
\end{aligned}\tag{20}
$$

where $\Big\langle A,B\Big\rangle=\mathrm{tr}\left(A^\top B\right)$ denotes the Frobenius inner product.

Define the lifted state error

$$E=\hat{X}X^{-1}=(\tilde{A},\tilde{a}),\tag{21}$$

where

$$\tilde{A} = \hat{A}A^{-1},$$
$$\tilde{a} = \hat{a} - \mathrm{Ad}_{\hat{A}A^{-1}}\, a.$$

The dynamics of E is given by

$$\dot{E} = (\dot{\tilde{A}}, \dot{\tilde{a}}), \tag{22}$$

where

$$\dot{\tilde{A}} = (\mathrm{Ad}_{\tilde{A}}(\hat{V}_\xi - V_\xi) - \Delta_1)\tilde{A},$$
$$\dot{\tilde{a}} = \Big[\mathrm{Ad}_{\tilde{A}}\, a, \mathrm{Ad}_{\hat{A}}(\hat{V}_\xi - V_\xi) - \Delta_1\Big] - \Delta_2.$$

Substituting Δ_1 and Δ_2 in (17),

$$\begin{aligned}\dot{\mathcal{L}} &= -\Big\langle k_1 \mathbb{P}_{\mathfrak{se}(3)}(M), M\Big\rangle \\ &= -k_1\Big\langle \mathbb{P}_{\mathfrak{se}(3)}(M), \mathbb{P}_{\mathfrak{se}(3)}(M)\Big\rangle \\ &= -k_1||\mathbb{P}_{\mathfrak{se}(3)}(M)||_F^2 \\ &= -k_1||\mathbb{P}_{\mathfrak{se}(3)}(\hat{A}^\top(I-\tilde{A})QA^{-\top})||_F^2, \end{aligned} \tag{23}$$

where $Q = \sum_{i=1}^{N} \frac{1}{N}\overline{p}_i^{\circ}\overline{p}_i^{\circ\top} + \hat{\overline{m}}^{\circ}\hat{\overline{m}}^{\circ\top}$, which is a symmetrical positive definite matrix if there are at least three non-collinear landmarks visible. This proves that the estimation error terms are bounded.

Computing the second time derivative of the Lyapunov function

$$\begin{aligned}\ddot{\mathcal{L}} = -k_1 \,\mathrm{tr}\Big(&(\mathbb{P}_{\mathfrak{se}(3)}(\hat{A}^\top(I-\tilde{A})QA^{-\top}))^\top \\ &(\mathbb{P}_{\mathfrak{se}(3)}(\dot{\hat{A}}^\top(I-\tilde{A})QA^{-\top} \\ &+ \hat{A}^\top(\dot{\tilde{A}})QA^{-\top} + \hat{A}^\top(I-\tilde{A})Q\dot{A}^{-\top}))\Big),\end{aligned}$$

where all the terms are bounded. Applying Barbalat's lemma, proves that $\dot{\mathcal{L}}$ converges asymptotically to zero, and hence

$$||\mathbb{P}_{\mathfrak{se}(3)}(\hat{A}^\top(I-\tilde{A})QA^{-\top})||_F^2 \to 0.$$

Let

$$\hat{A} = \begin{bmatrix}\hat{R}_A & \hat{t}_A \\ 0 & 1\end{bmatrix}, \quad A = \begin{bmatrix}R_A & t_A \\ 0 & 1\end{bmatrix},$$
$$Q = \begin{bmatrix}\Sigma & \mu \\ \mu^\top & 1\end{bmatrix}, \qquad \tilde{A} = \begin{bmatrix}\tilde{R}_A & \tilde{t}_A \\ 0 & 1\end{bmatrix}.$$

then

$$\mathbb{P}_{\mathfrak{se}(3)}(\hat{A}^\top(I-\tilde{A})QA^{-\top}) = \mathbb{P}_{\mathfrak{se}(3)}\Big(\begin{bmatrix}S_{11} & S_{12} \\ (\cdot) & (\cdot)\end{bmatrix}\Big),$$

where $(\cdot)$ represent the part of the matrix that does not matter, and

$$\begin{aligned}S_{11} &= \hat{R}_A{}^\top(I-\tilde{R}_A)(\Sigma R_A - \mu t_A{}^\top R_A) \\ &\quad - \hat{R}_A{}^\top\tilde{t}_A(\mu^\top R_A - t_A{}^\top R_A), \\ S_{12} &= \hat{R}_A{}^\top(I-\tilde{R}_A)\mu - \hat{R}_A{}^\top\tilde{t}_A.\end{aligned}$$

So,

$$\tilde{t}_A = (I-\tilde{R}_A)\mu, \tag{24}$$

$$\mathbb{P}_{\mathfrak{so}(3)}(S_{11}) = \frac{R_A{}^\top(\tilde{R}_A{}^\top\bar{Q} - \bar{Q}\tilde{R}_A)R_A}{2} = 0, \tag{25}$$

where

$$\bar{Q} = \Sigma - \mu\mu^\top.$$

From (25), we have

$$\tilde{R}_A{}^\top\bar{Q} = \bar{Q}\tilde{R}_A.$$

Following the proof of Theorem 5.1 in (Mahony et al., 2008), $\tilde{R}$ is asymptotically stable to I. From (24), $\tilde{t}_A$ is asymptotically stable to 0. Thus, $\tilde{A}$ is asymptotically stable to I, regardless of the choice of ξ°. □

Note that the observer is implementable without requiring body-fixed linear and angular velocity.

5. EXPERIMENTAL RESULTS

We evaluate the performance of our proposed observer with the help of simulation. We tested for two separate scenarios – (1) the case where the device has multiple accelerometers placed at known locations (similar to Ng et al. (2019)) such that both the linear and angular acceleration can be measured, (2) the case where one accelerometer and one gyroscope is installed on the device, which is a more common sensor configuration.

In the simulation, there are 12 landmarks randomly generated on two planar ($12\times12m^2$) surfaces orthogonal to each other, which represents known landmarks (e.g., ArUco markers) placed on walls in a room. The simulated vision sensor (landmark data) has a sampling frequency of $30Hz$ and field of view of 90°. A consequence of this choice is that all landmarks are not visible at all times. We implement the proposed algorithm for all visible landmarks and note that this will cause discontinuities in the evolution of the Lyapunov function (Figure 2 and 4) as landmarks enter or leave the field of view.

The simulated magnetic field is in the direction $[1,0,0]^\top$, and gravity vector is $[0,0,9.81]ms^{-2}$. The simulated IMU has a sampling frequency of $200Hz$ and the observer state is updated at $1000Hz$. The simulated noise for all sensor measurements follows a zero mean Gaussian process, with standard deviation of 0.03 along each axis. Note that our observer does not rely on the Gaussian noise assumption.

The device is undergoing a smooth sinusoidal motion with linear and angular velocity vector following the function $[0.25sin(0.1t+2); -0.025; -0.25cos(0.1t-3)]$ and $[sin(0.05t); cos(0.05t); 0]$.

We have also implemented an EKF using 13 state variables, where the orientation is represented with a quaternion. The gains of our observer is tuned such that the rate of convergence is similar to the EKF for a fairer comparison. The following subsections present the simulation results for the two sensor configurations.

5.1 Simulation with Measured Linear and Angular Acceleration

From (5), the input angular acceleration $\theta^\times$ is measured using an array of accelerometers placed at known location similar to that described in (Ng et al., 2019). The input linear acceleration follows (4), where the state variables P_ξ, Ω and v are replaced with the estimate $\hat{P}_\xi$, $\hat{\Omega}$ and $\hat{v}$, such that

$$\hat{\tilde{a}}_B = \hat{\tilde{a}} - \hat{P}_\xi{}^{-1}\hat{\tilde{a}}_G - \hat{\Omega}\times\hat{v}. \tag{26}$$

Figure 1 shows the time evolution of the error in pose P_ξ and velocity V_ξ converging asymptotically to zero. Figure 2 shows the time evolution of the Lyapunov function $\mathcal{L}$ asymptotically converging to zero.

From Figure 1, we can observe that the EKF performs similar to our observer in the simulation. It can also be noted that the EKF method requires higher memory and computational requirements than our proposed observer, where large covariance and Jacobian matrices have to be computed. EKF also relies on the Gaussian noise assumption, and requires prior knowledge of the covariance matrices of the process and measurement noise, which are not required by our observer.

The jumps in the evolution of the Lyapunov function in the first 5 seconds of Fig. 2 are associated with landmarks entering and leaving the field of view. The strong asymptotic convergence properties ensure that these small transients are quickly compensated for in the observer state. Once the principle observer state transient is complete, after around 10s, the effect of new image points entering the field of view becomes insignificant.

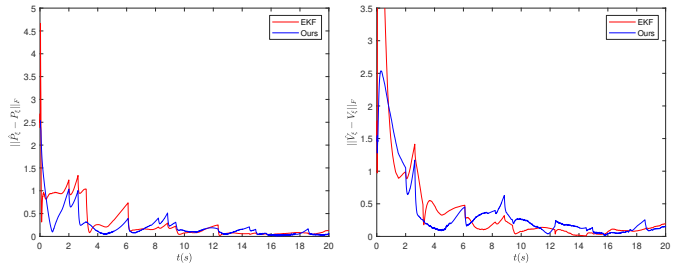

Fig. 1. Time evolution of pose P_ξ and velocity V_ξ error showing asymptotic convergence and practical stability in the presence of noise.

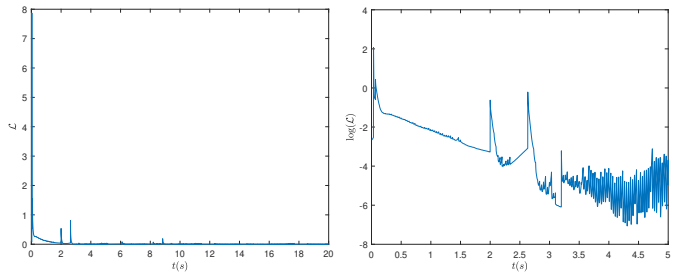

Fig. 2. Time evolution of the Lyapunov function $\mathcal{L}$ showing asymptotic convergence to practical stability.

5.2 Simulation with Measured Linear Acceleration and Angular Velocity

In this simulation set-up, we consider the case where the angular acceleration is not measured. In this case, we replace $\hat{\Omega} = \Omega$ the measurement of angular velocity in the pose velocity estimate $\hat{V}$. In the absence of a measurement of angular acceleration θ we use a low pass filtered numerical derivative of the measured gyroscope, such that at time instance k,

$$\theta_k \approx 0.2\theta_{k-1} + 0.8\frac{\mathrm{d}}{\mathrm{d}t}\Omega_k, \tag{27}$$

in the definition of U_2 for (17). The additional noise injected into the velocity estimate will not affect the angular velocity since the state of the estimator is directly set to the measurement. However, the derivative estimate is important in modelling the coupling due to the semi-direct product in the group structure.

Figure 3 shows the time evolution of the error in pose P_ξ and velocity V_ξ converging asymptotically to zero. Figure 4 shows the time evolution of the Lyapunov function $\mathcal{L}$ asymptotically converging to zero.

From Fig. 3, it can be seen that our observer and EKF performs similarly. It can be observed that the estimated pose and velocity is noisier than the case where the angular acceleration is directly measured by multiple accelerometers. This is due to the additional noise introduced by the numerical derivative of the noisy gyroscope measurement, which affects the estimated linear velocity due to the coupling effect. From the logarithm of the Lyapunov in Fig. 2 and 4, it can be observed that the jumps at $2s$ and $3.2s$ are present in both plots, due to significant changes in the visible landmarks. The logarithm of the Lyapunov plots also shows clear linear decreasing trend, which is a characteristic of exponential convergence of the Lyapunov function to zero.

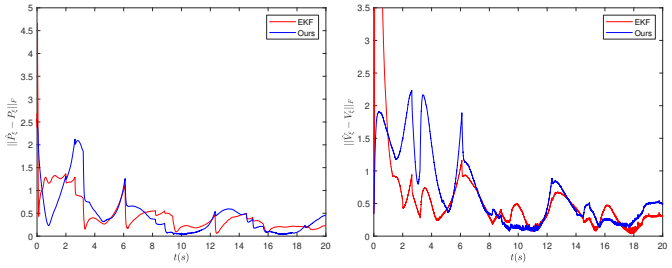

Fig. 3. Time evolution of pose P_ξ and velocity V_ξ error showing asymptotic convergence and practical stability in the presence of noise.

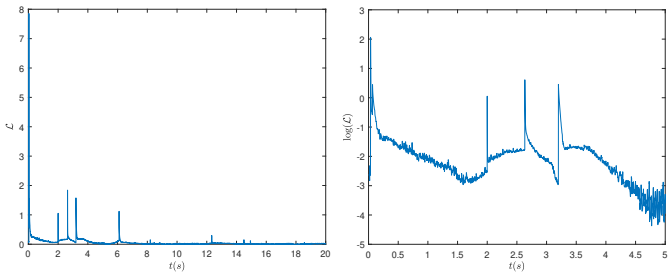

Fig. 4. Time evolution of Lyapunov function $\mathcal{L}$ showing asymptotic convergence to practical stability.

6. CONCLUSIONS

An equivariant observer for the second order pose kinematics was presented. The observer does not rely on the measurement of linear velocity commonly used by existing methods. The observer works on the symmetry group of the second order pose state space, and is shown to exhibit strong asymptotic convergence property, regardless of the chosen origin point $(P_{\xi^\circ}, V_{\xi^\circ})$.

Future work includes the study of sensor bias, and more experimental validation on actual hardware for VR or AR applications.

REFERENCES

Baldwin, G., Mahony, R., and Trumpf, J. (2009). A nonlinear observer for 6 dof pose estimation from inertial and bearing measurements. In *2009 IEEE International Conference on Robotics and Automation*, 2237–2242. IEEE.

Barrau, A. and Bonnabel, S. (2016). The invariant extended kalman filter as a stable observer. *IEEE Transactions on Automatic Control*, 62(4), 1797–1812.

Bonnable, S., Martin, P., and Salaün, E. (2009). Invariant extended kalman filter: theory and application to a velocity-aided attitude estimation problem. In *Proceedings of the 48h IEEE Conference on Decision and Control (CDC) held jointly with 2009 28th Chinese Control Conference*, 1297–1304. IEEE.

Brockett, R. and Sussmann, H. (1972). Tangent bundles of homogeneous spaces are homogeneous spaces. *Proceedings of the American Mathematical Society*, 35(2), 550–551.

Grip, H.F., Fossen, T.I., Johansen, T.A., and Saberi, A. (2011). Attitude estimation using biased gyro and vector measurements with time-varying reference vectors. *IEEE Transactions on Automatic Control*, 57(5), 1332–1338.

Hamel, T. and Samson, C. (2017). Riccati observers for the nonstationary pnp problem. *IEEE Transactions on Automatic Control*, 63(3), 726–741.

Hashim, H.A., Brown, L.J., and McIsaac, K. (2019). Nonlinear stochastic position and attitude filter on the special euclidean group 3. *Journal of the Franklin Institute*, 356(7), 4144–4173.

Hua, M.D., Ducard, G., Hamel, T., Mahony, R., and Rudin, K. (2014). Implementation of a nonlinear attitude estimator for aerial robotic vehicles. *IEEE Transactions on Control Systems Technology*, 22(1), 201–213.

Hua, M.D., Hamel, T., Mahony, R., and Trumpf, J. (2015). Gradient-like observer design on the special euclidean group se (3) with system outputs on the real projective space. In *2015 54th IEEE Conference on Decision and Control (CDC)*, 2139–2145. IEEE.

Hua, M.D., Hamel, T., and Samson, C. (2017). Riccati nonlinear observer for velocity-aided attitude estimation of accelerated vehicles using coupled velocity measurements. In *2017 IEEE 56th Annual Conference on Decision and Control (CDC)*, 2428–2433. IEEE.

Hua, M.D., Martin, P., and Hamel, T. (2016). Stability analysis of velocity-aided attitude observers for accelerated vehicles. *Automatica*, 63, 11–15.

Hua, M.D., Zamani, M., Trumpf, J., Mahony, R., and Hamel, T. (2011). Observer design on the special euclidean group se (3). In *2011 50th IEEE Conference on Decision and Control and European Control Conference*, 8169–8175. IEEE.

Hua, M.D. and Allibert, G. (2018). Riccati observer design for pose, linear velocity and gravity direction estimation using landmark position and imu measurements. In *2018 IEEE Conference on Control Technology and Applications (CCTA)*, 1313–1318. IEEE.

Hughes, C.E., Stapleton, C.B., Hughes, D.E., and Smith, E.M. (2005). Mixed reality in education, entertainment, and training. *IEEE computer graphics and applications*, 25(6), 24–30.

Liu, S.Q. and Zhu, R. (2018). A complementary filter based on multi-sample rotation vector for attitude estimation. *IEEE Sensors Journal*, 18(16), 6686–6692.

Mahony, R., Hamel, T., and Pflimlin, J.M. (2008). Nonlinear complementary filters on the special orthogonal group. *IEEE Transactions on automatic control*, 53(5), 1203–1217.

Mahony, R., Hamel, T., Trumpf, J., and Lageman, C. (2009). Nonlinear attitude observers on so (3) for complementary and compatible measurements: A theoretical study. In *Proceedings of the 48h IEEE Conference on Decision and Control (CDC) held jointly with 2009 28th Chinese Control Conference*, 6407–6412. IEEE.

Mahony, R., Trumpf, J., and Hamel, T. (2013). Observers for kinematic systems with symmetry. *IFAC Proceedings Volumes*, 46(23), 617–633.

Marchand, E., Uchiyama, H., and Spindler, F. (2015). Pose estimation for augmented reality: a hands-on survey. *IEEE transactions on visualization and computer graphics*, 22(12), 2633–2651.

Ng, Y., van Goor, P., Mahony, R., and Hamel, T. (2019). Attitude observation for second order attitude kinematics. In *2019 58th IEEE Conference on Decision and Control*. IEEE.

Rabbi, I. and Ullah, S. (2013). A survey on augmented reality challenges and tracking. *Acta graphica: znanstveni časopis za tiskarstvo i grafičke komunikacije*, 24(1-2), 29–46.

Wu, K., Zhang, T., Su, D., Huang, S., and Dissanayake, G. (2017). An invariant-ekf vins algorithm for improving consistency. In *2017 IEEE/RSJ International Conference on Intelligent Robots and Systems (IROS)*, 1578–1585. IEEE.

Appendix A. LEFT TRANSLATION

Define the left translation on the group by $L_X : \mathbf{G} \to \mathbf{G}$, $L_X Y := X \cdot Y$.

Define a map $\mathrm{d}L_X : \mathrm{T}_I\mathbf{G} \to \mathrm{T}_X\mathbf{G}$ by

$$\mathrm{d}L_{(A,a)}[w_1, w_2] = (Aw_1, \mathrm{Ad}_A\, w_2).$$

Lemma A.1. $\mathrm{d}L_{(A,a)}$ is the differential of the left translation $L_{(A,a)}$.

Proof. Computing the differential of the left translation

$$\begin{aligned}
&\mathrm{D}_{(B,b)}\Big|_{I,0}((A,a)\cdot(B,b))[w_1,w_2] \\
&\quad = \mathrm{D}_{(B,b)}\Big|_{I,0}(AB, a + \mathrm{Ad}_A\, b)[w_1,w_2] \\
&\quad = (Aw_1, \mathrm{Ad}_A\, w_2) \\
&\quad = \mathrm{d}L_{(A,a)}[w_1,w_2].
\end{aligned}$$

□